Science of the Total Environment 787 (2021) 147720

Contents lists available at ScienceDirect

Science of the Total Environment

journal homepage: www.elsevier.com/locate/scitotenv

Evaluation of select biochars and clays as supports for phytase to increase the fertilizer potential of animal wastes

Chongyang Li [a,*], Zhengyang Wang [b], Santanu Bakshi [b,1], Joseph J. Pignatello [b], Sanjai J. Parikh [a]

[a] Department of Land, Air and Water Resources, University of California, Davis, CA 95616, USA
[b] Department of Environmental Sciences, The Connecticut Agricultural Experiment Station, New Haven, CT 06511, USA

HIGHLIGHTS

- Phytase is effectively bound by physisorption with no need for covalent grafting.
- Phytase loading rate is largely influenced by pH and biochar aromatic content.
- Phytase binding was irreversible even in high concentrations of manure extract.
- Binding to biochars reduces phytase activity more so than clay mineral tested.

GRAPHICAL ABSTRACT

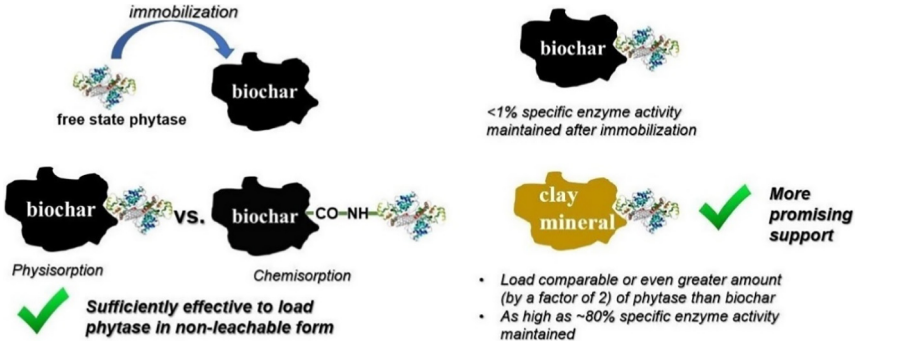

ARTICLE INFO

Article history:
Received 11 January 2021
Received in revised form 6 May 2021
Accepted 8 May 2021
Available online 13 May 2021

Editor: Jay Gan

Keywords:
Enzyme immobilization
Organophosphates mineralization
Manure
Physisorption
Covalent grafting

ABSTRACT

Manures may contain considerable amounts of organophosphates (org-P) that must be enzymatically converted to inorganic phosphate (i.e., PO_4-P) to be plant available. Although adding enzymes into manures can facilitate mineralization of org-P to PO_4-P, enzymes that are not immobilized are easily lost through leaching, degradation, or denaturation. In this study, the immobilization of enzymes onto nine different biochar surfaces was explored. Phytase, which mineralizes a main class of org-P, was used as the model enzyme. Immobilization methods included covalent grafting accomplished by the carbodiimide crosslinker method and physical sorption. The results showed that physisorption was as effective as grafting for loading phytase to the biochars. Phytase loading after mixing 0.1 g biochar and 2 mg phytase correlated positively with biochar C:H ratio (an indicator of aromatic content) suggesting the importance of the hydrophobic effect. An increase in pH led to a decrease in phytase loading consistent with repulsion between negatively charged sites on phytase and the increasing negative charge on biochar. Less than 4% of the immobilized phytase leached after sequential extractions over seven days using manure dissolve organic matter solutions. However, the activity of immobilized phytase decreased markedly compared to the free state phytase. The specific activity of immobilized phytase was two orders of magnitude lower than that of free phytase at pH 5 and 7. Nevertheless, results showed that deactivation of phytase by biochars were reversible once the phytase was detached from the surfaces. Compared to the biochars, clay minerals (montmorillonite, kaolinite and hematite) tended to have greater loading rates and higher phytase activity. Composting manures with coamendments of biochar and minerals may enhance both short- and long-term P mineralization potential.

Published by Elsevier B.V.

* Corresponding author at: Crop Sciences, University of Illinois, Urbana-Champaign, IL 61801, USA.
E-mail address: cyfli@ucdavis.edu (C. Li).
[1] Bioeconomy Institute, Iowa State University, Ames, IA 50011, USA.

https://doi.org/10.1016/j.scitotenv.2021.147720
0048-9697/Published by Elsevier B.V.

1. Introduction

Animal manures are nutrient-rich organic materials that can supply crops with multiple nutrients, including nitrogen (N) and phosphorus (P) (Jensen, 2013). However, inorganic and organic compositions of manures can vary drastically. For example, organic P in manure varies from 10 to 80% of total P, and becomes plant-available only after mineralization to inorganic P (Barnett, 1994; Tarafdar and Claassen, 1988). Therefore, it is recommended to investigate the composition of the manure and estimate the mineralization rates of the organic nutrients before the amount of manure needed to satisfy the nutrient requirements of crops can be determined. Estimation of the mineralization process, however, is challenging because it is influenced by multiple factors, including manure properties (e.g., type, age), soil properties (e.g., texture, organic matter content), and the soil environment (e.g., pH, moisture, temperature) (Araji et al., 2001). Inaccurate mineralization rate estimates often lead to over-application or repeated application of animal manure, increasing the risks of nutrient runoff and leaching which are of environmental concern (Abdala et al., 2012; Jongbloed and Lenis, 1998; Kleinman et al., 2015).

Mineralization of organic nutrients prior to manure application—for example, during composting—can ensure nutrients are in a plant-assimilable form and the manure is applied at the appropriate rate. Deployment of enzymes in their free form on an industrial scale, however, is often hampered by their low stability and high leachability (Hartmann and Kostrov, 2013), sensitivity to denaturation by the operational conditions (e.g., pH, temperature changes), and loss of activity due to microbial degradation (Hudson et al., 2005; Mohamad et al., 2015). Immobilization of enzymes onto a solid support provides an attractive approach to overcoming these obstacles (Guzik et al., 2014; Khan and Alzohairy, 2010). Enzyme immobilization has become a cost-effective solution in water/soil bioremediation, energy production (e.g., biodiesel synthesis), biomedical applications, and food processing (Liang et al., 2000; Panesar et al., 2010; Ranganathan et al., 2008; Sharma et al., 2018).

Biochar, a material derived from the pyrolysis of residual biomass, is discussed as an alternative to other materials traditionally considered for use as enzyme supports, such as clay, silica, polymers, metal oxides and carbon. Biochar shows desirable characteristics, including high surface area, insolubility, high chemical stability, resistance to biological decay, and relatively low cost (Almeida et al., 2017; Quirós et al., 2011). Studies have reported enhanced activity of immobilized lipase (González et al., 2013; Khosla et al., 2017), lysozyme (Noritomi et al., 2012; Vinu et al., 2005), and laccase (Naghdi et al., 2017; Taheran et al., 2017) immobilized on biochar. Other studies have reported highly variable effects of biochar on enzyme activity, depending on soil properties and enzyme types (Bailey et al., 2011; Elzobair et al., 2016; Khadem and Raiesi, 2019). For example, enhanced phosphatase and β-glucosidase activities are often found after applying biochars in soils polluted by heavy metals like Pb or Ni (Naeem et al., 2021; Turan, 2019; Turan, 2020), but reduced leucine aminopeptidase and β-xylosidase activities were reported in a non-polluted agricultural soil (Elzobair et al., 2016). However, no studies have been reported on immobilization of enzymes onto biochars for purposes of mineralizing organic nutrients in manure before fertilizing the soil. Biochar is of current interest as a soil amendment to improve soil quality and nutrient retention (Hagemann et al., 2017; Jones et al., 2012), or combined with other immobilizing agents (e.g., clays and cements) to remediate polluted soil (Shahbaz et al., 2019; Turan et al., 2018a; Turan et al., 2018b). The use of immobilized phytase on biochar as an add-mixture with manure thus potentially confers added value to the biochar.

Immobilization of enzymes can be accomplished by reversible and irreversible means, represented by physical adsorption (physisorption) and covalent binding (grafting), respectively (Brena and Batista-Viera, 2006). Physisorption is simple to achieve and only requires the material have a high surface area. While it offers greater chance for preserving enzyme activity, leaching can be of concern (Nguyen et al., 2016). By contrast, grafting is irreversible, but is more prone to inducing conformational changes in the enzyme that can lead to significant loss of activity, and the cross-linking procedure may be expensive (Kazenwadel et al., 2015). Biochars are suitable materials for either physisorption or grafting approaches since they can be made with high surface area and an abundance of —OH and —COOH groups on their surfaces (Igalavithana et al., 2017).

The primary objective of this study was to screen a variety of biochars for their ability to bind phytase in non-leachable form in comparison with soil clay minerals, which are endogenous components in soil and commonly used enzyme immobilization supports. Enzymatic activities of the immobilized phytase were also examined to determine the optimal enzyme grafting support.

2. Materials and methods

2.1. Chemicals

Phytase (extracted from wheat), enzyme assay substrate (*p*-nitrophenyl phosphate, or *p*NPP), enzymatic reaction product (*p*-nitrophenol, or *p*NP), phytase grafting cross-linker (1-ethyl-3-(3-dimethylaminopropyl) carbodiimide, or EDC), and protein assay kit (Bovine serum albumin standard and Bradford reagent) were from Sigma Aldrich. Carboxylic resin with size of 100–200 mesh and containing 1.11 mmol g^{-1} —COOH groups (used for estimating the contribution of covalent bonding in phytase immobilization, Section 2.3) was from ChemPep Inc. The buffer solution used for phytase immobilization (Section 2.3) and enzymatic activity determination (Section 2.4) was a modified universal buffer (MUB), consisting of boric acid, citric acid, maleic acid, and 2-amino-2 (hydroxymethyl)-1–3-propanediol (THAM or Tris Base) (Turner, 2010). This buffer was chosen because there is no phosphate component and it allows the assessment of pH profiles over a wide pH buffer range (pH of MUB can be adjusted by addition of HCl or NaOH). The components in the MUB and all other chemicals not already specified were from Fisher Scientific. Dairy and poultry manure water-extractable matter was obtained from manures generated by local farms near Davis, California. Details of the manure extraction procedure and the characteristics of the manure extracts are described in a previous study (Wang et al., 2020). Kaolinite, montmorillonite, and hematite were obtained from Ward's Science.

2.2. Biochars and biochar characterization

Nine biochars from different feedstocks and production methods were obtained from various suppliers (Table 1). All biochars were air-dried and ground and sieved to a size range of 0.1–0.5 mm. Post-pyrolysis air oxidation (PPAO) treatment was performed on the nine raw biochars, as it effective for increasing —COOH and —OH content of biochars (Xiao and Pignatello, 2016). The PPAO treatment was conducted in the same manner previously described (Xiao et al., 2018; Xiao and Pignatello, 2016): briefly, 0.1 g of raw biochar was placed in a cylindrical shaped vial and heated in a muffle furnace at 400 °C in an air atmosphere for 40 min. The PPAO-treated biochars were used to optimize the phytase loading rate in only one subset of experiment (details in Section 2.3).

The C, H, O and N contents of the biochars were determined with a Costech ECS 4010 using acetanilide as the calibration standard. The pH and electrical conductivity (EC) were measured in 18.2 MΩ·cm water using a 1:10 ratio (*w*/*v*) with stirring and an equilibration time of 1 h (Orion 4 Star, Thermo Fisher Scientific). Dissolved organic carbon (DOC) was determined by sequentially extracting the biochars with 18.2 MΩ·cm water (w/v, 1:50) until no DOC was detected (detection limit: 25 μg L^{-1}). The extracts were acidified with HCl and non-volatile OC was measured by a TOC-VCSH analyzer (Shimadzu, Canby) using potassium hydrogen phthalate as the calibration standard. Surface

Table 1
Biochar production information.

	Feedstock	Production method	HTT (°C)	RT at HTT	Supplier
B1	Walnut shell	Gasification	800–900	4 h	Dixon Ridge Farm, CA
B2	Mixed fir and pine wood	Fast pyrolysis	865	20 s	Oregon Biochar Solutions, OR
B3	Softwood forestry residue	Fast pyrolysis	800	<1 min	Pacific Biochar, CA
B4	Maple wood	Slow pyrolysis	500	2 h	Connecticut Agricultural Experiment Station, CT
B5	Almond shell and sawdust	Hydro pyrolysis	400–500	20 min	The Kerr Center, OK
B6	Cedar sawdust	Hydro pyrolysis	400–500	20 min	The Kerr Center, OK
B7	Pine wood	Slow pyrolysis	900	4 h	UC Davis, CA
B8	Pine wood	Slow pyrolysis	500	4 h	UC Davis, CA
B9	Pine wood	Slow pyrolysis	500	2 h	Connecticut Agricultural Experiment Station, CT

Abbreviations: HTT, highest treatment temperature; RT, residence time.

area was measured by CO_2 porosimetry at 273.15 K. Approximately 50 mg of biochar was outgassed at 200 °C for at least 8 h and then analyzed on an Autosorb iQ Analyzer (Quantachrome Instruments). Data points with relative pressures of ~4×10^{-7}–~3×10^{-2} were used to calculate the surface area via software Quantachrome ASiQwin (version 5.21) based on density functional theory. Carboxylic acid groups were quantified via the modified Boehm titration method (Fidel et al., 2013). Electrokinetic (zeta) potentials were measured on ZetaPlus (Brookhaven Instruments Corp.) at a biochar: water ratio of 100 mg: 200 mL. An aliquot of the suspension was adjusted with HCl/NaOH to the desired pH (4.0–7.0) or NaCl to the desired EC (10–40 mS cm^{-1}) and magnetically stirred to equilibrate before measurement. Total metal concentrations were determined after digestion with 70% HNO_3 at a solid-to-acid ratio of 50 mg:10 mL in a closed vessel at 170 °C for 8 h. The digestates were filtered (Whatman 589/3) and diluted before analysis on an Agilent 7900 inductively-coupled-plasma mass spectrometry (ICP-MS) (Agilent Technologies).

2.3. Immobilization methods and phytase loading rate measurements

This study considered both "irreversible" (grafting) and "reversible" (physisorption) methods for phytase immobilization. For the grafting method, —COOH groups on biochars were coupled using a carbodiimide cross-linker (EDC) to a free —NH_2 in phytase to form an amide bond (biochar-CO-NH-enzyme) (Novick and Rozzell, 2005). The physisorption approach was performed by simply mixing biochar and phytase under the same conditions but in absence of EDC ("no EDC control"). Details are provided in Text S1. Four factors, leading to four subsets of experiments, were examined for their effects on phytase loading: pH, EDC dose, —COOH content (achieved by comparing raw char and PPAO-treated char) and EC (an index of ionic strength). The experimental matrix is shown in Table 2.

Initially, 0.1 g of biochar was placed in 10 mL of buffer with 2 mg solubilized phytase. The protein concentration in the initial and final solutions was determined spectrophotometrically at 595 nm based on the Bradford dye-binding procedure (Bradford, 1976). Bovine serum albumin (0 to 0.2 mg protein mL^{-1}) was used as the calibration standard. The mass of immobilized phytase was calculated by subtracting the protein mass remaining in the solution after removal of the solid by filtration, from the initial protein mass in the reaction mixture. Phytase-treated biochars were dried in a gentle flow of N_2 gas and stored in amber bottles at 4 °C.

Immobilization of phytase on carboxylic resin by grafting was performed in the same manner as for the biochars.

2.4. Detachment of immobilized phytase from biochar surface

2.4.1. Leaching of immobilized phytase from biochar

Aqueous solutions of dairy and poultry manure water-extractable matter (details in Wang et al. (2020)) were used to simulate the potential leaching of immobilized phytase from biochar surfaces. Phytase/biochar biocatalyst (0.1 g) was sequentially extracted seven times, each time lasting 24 h, with 10 mL solution at 4 °C in the dark with continuous shaking. After each extraction, the vessel was centrifuged to separate the solid and solution phases and the protein concentration in the supernatant was quantified. The solution phase was then replaced with a 10-mL portion of fresh solution in the same tube and the next extraction step performed. Cumulative protein loss was calculated by summing the protein solubilized after each extraction.

2.4.2. Re-mobilization of phytase from biochar using exhaustive extraction

Preliminary tests showed that five-times sequential extraction with 10% (v/v) ethanol in 1 M NH_4Cl with sonication was the best of several methods for extracting physisorbed immobilized phytase from biochars, giving recoveries of 31–49% (details in Text S2 and Table S1).

Table 2
Optimization experiments of the phytase immobilizations to maximize phytase loading.

	pH	EDC: biochar mass ratio	—COOH content	EC
Part I: buffer pH[a]	4.0 5.0 6.0 7.0	0 (adsorption) 0.5 (covalent binding)	Raw chars only (low —COOH)	10 mS cm^{-1}
Part II: EDC dosage	5.0	0 (adsorption) 0.5 (covalent binding) 1.0 (covalent binding) 1.5 (covalent binding)	Raw chars only (low —COOH)	10 mS cm^{-1}
Part III: —COOH content	5.0	0 (adsorption) 0.5 (covalent binding)	Raw chars (low —COOH) PPAO chars (high —COOH)	10 mS cm^{-1}
Part IV: buffer EC[b]	5.0	0 (adsorption)	Raw chars only (low —COOH)	10 mS cm^{-1} 20 mS cm^{-1} 40 mS cm^{-1}

[a] Buffer pH is adjusted to target using NaOH or HCl.
[b] Buffer EC is adjusted to target using NaCl.

Phytase obtained from this process is hereafter referred to as re-mobilized phytase.

2.5. Enzymatic activities of free, immobilized, and re-mobilized phytases

Catalytic activity of the phytase was determined spectrophotometrically using para-nitrophenyl phosphate (*p*NPP) as a substrate. One milligram phytase protein, either in free form or immobilized, was mixed with 5 mL substrate (ranging from 5 to 200 mM to generate a rate curve) buffered with MUB at pH 5 or 7, which represents two agricultural soil-relevant pH conditions. The EC of the buffer was adjusted to 10 mS cm^{-1} by addition of NaCl. The mixture was incubated for 1 h at 25 °C, and the enzymatic reaction was terminated with 5 mL 0.2 M NaOH, followed by measuring the absorbance of the product *p*NP at 410 nm. Since biochars showed strong affinity towards *p*NP, an extra step of extracting *p*NP with acetonitrile at 60 °C was performed (details in Text S3) (Yang et al., 2017). For reactions with low enzymatic activity, *p*NP was concentrated via freeze-drying and reconstituted with water to be above the detection limit. The Michaelis-Menten constant K_m and the maximum reaction velocity V_{max} for the free and immobilized phytase were calculated by:

$$\frac{1}{v} = \frac{K_m}{V_{max}}\frac{1}{[p\mathrm{NPP}]} + \frac{1}{V_{max}}$$

where v is the reaction rate at each [*p*NPP].

To determine whether the extraction conditions used to obtain re-mobilized phytase (Section 2.4.2) caused a loss of phytase activity, free-state phytase was subjected to the extraction conditions (sonicating in 10% ethanol in 1 M NH_4Cl) and the resulting enzymatic activity (at a single substrate level of 200 mM) compared with that of the free state not subjected to those conditions.

2.6. Immobilization of phytase on minerals

Only the physisorption method (EDC-free) was used to attach phytase to kaolinite, montmorillonite, and hematite. The conditions were: 2 mg phytase, 0.1 g mineral, 10 mL MUB (pH 5), EC of 10 mS cm^{-1}, and 24 h equilibration. Phytase loading and immobilized phytase activity were determined the same as in Sections 2.3 and 2.5, respectively. The assay pH values were, again, 5 and 7. The enzymatic activities was measured at a single substrate level of 200 mM.

2.7. Statistics

All measurements were conducted in triplicate and statistical analyses were performed using JMP (Version 12.1). For each measured property (e.g., phytase loading rate), ANOVA was first performed using an exploratory model to test for potential interactions between factors, if more than one ($p < 0.05$). If a significant interaction was found, effects were analyzed separately; otherwise, comparison was performed together. Measured properties were analyzed for differences at 5% significance using the Tukey test. Shapiro-Wilks and Levene's tests were used to verify the normality and homogeneity of variance assumptions required by ANOVA with transformation (logarithm) performed if needed.

3. Results

3.1. Biochar and phytase characteristics

Select physio-chemical properties of the nine raw biochars are listed in Table 3. Carbon content was above 60% except for B3, and H content ranged from 0.3 to 3.6%, leading to a C:H ratio ranging from 1.7:1 to 17.6:1. All raw biochars were alkaline (pH > 8) but the EC varied widely. Enzyme assays for immobilized phytases on B5 or B6 were not conducted because absorbance from DOC was so strong it interfered with *p*NP determination. Specific surface area differed greatly (191–972 m^2 g^{-1}), and —COOH content ranged from 0.15 to 0.41 mmol g^{-1} among the biochars. Zeta potential measurements indicated that all biochars were negatively charged above pH 4, and for most biochars, the zeta potential became more negative monotonically with increasing pH in the measured range (Table 4). Common metals in these biochars included Fe, Mn, Cu and Zn, with others at trace levels (Table 5). The Mn, Cu and Zn contents were relatively high for B3, B7 and B8.

Table 3
Physical-chemical properties of biochars.

	C (%)	H (%)	O (%)	N (%)	pH	EC (mS cm^{-1})	DOC (g kg^{-1})	Surface area (m^2 g^{-1})	Carboxyl content (mmol g^{-1})
B1	63.3	0.3	8.9	0.54	10.4	4.32	1.49	772.6	0.25
B2	62.7	1.5	6.0	0.27	10.7	2.33	1.35	972.2	0.33
B3	47.6	0.9	10.2	0.16	10.4	2.38	1.17	662.7	0.33
B4	79.1	2.6	7.4	0.22	8.1	0.16	2.48	652.8	0.22
B5	61.4	3.1	16.5	0.64	9.7	3.17	40.1	190.9	0.41
B6	70.4	3.6	20.1	0.16	8.0	2.03	44.4	395.2	0.15
B7	92.4	0.5	8.8	0.13	10.6	0.22	1.15	839.1	0.19
B8	81.7	1.6	6.1	0.46	10.1	0.13	1.05	661.8	0.17
B9	82.2	2.9	7.5	0.17	9.4	0.11	2.61	629.4	0.16
B1-PPAO	60.4	0.2	18.6	0.25	9.1	1.01	1.05	827.4	0.29
B2-PPAO	61.4	1.2	9.0	0.21	10.3	2.76	1.18	1043.6	0.55
B3-PPAO	46.3	0.5	15.5	0.18	10.7	4.00	0.84	807.8	0.42
B4-PPAO	74.7	2.6	20.4	0.2	4.5	0.19	1.14	817.9	0.83
B5-PPAO	50.9	2.1	22.2	0.49	5.9	2.95	16.7	429.4	0.45
B6-PPAO	59.3	2.6	29.4	0.10	5.1	2.77	21.3	444.5	1.29
B7-PPAO	86.3	0.4	12.6	0.11	9.0	0.75	0.99	739.3	0.21
B8-PPAO	63.8	1.1	19.1	0.38	8.1	0.62	0.61	534.9	0.64
B9-PPAO	66.9	2.7	22.7	0.35	7.2	0.29	1.57	673.2	0.60

Abbreviations: EC, electrical conductivity; DOC, dissolved organic carbon; B1–B9 biochar: refer to Table 1.

Biochar PPAO treatment led to a decrease in C, an increase in O, and a slight decrease in H contents (Table 3). The increase in —COOH content after PPAO was consistent with the increases in O content and titration acidity. PPAO treatment burned off some portion of the biochar, causing a decrease in DOC content while causing an increase in specific surface area (increases of 7–125% compared to the corresponding raw char, except B7 and B8). The trend of zeta potential with pH, however, was not affected by PPAO treatment.

The isoelectric point of phytase was between pH 5 and 6 (Table S2). The calculated mean diameter of phytase was 3.5 nm when dissolved in water and grew larger as the EC increased (Table S2). The diameter almost doubled when the EC increased from 10 to 40 mS cm^{-1}.

3.2. Phytase loading and reversibility

Experiments to optimize for phytase loading gave similar results for all nine biochars which can be summarized as follows. 1) Cross-linking using the carbodiimide EDC did not significantly increase phytase loading compared to the respective control, even at the highest EDC dose (Fig. S2). 2) The pH had a significant effect on phytase loading (Fig. 1). Phytase attachment decreased as the pH changed from 5 to 6 for most biochars. 3) PPAO treatment increased phytase loading by18–45% for some biochars (B1, B2, B7 and B8); but despite an increase in —COOH group content by PPAO (Table 3), EDC did not improve phytase loading (Fig. S3). 4) An increase in EC led to a decrease in phytase loading; the decrease was more significant when EC was increased from 10 to 20 mS cm^{-1} (Fig. S4). Based on these findings, the following conditions were chosen to achieve a high loading of phytase onto biochars using minimum labor and costs: pH of 5; EC of 10 mS cm^{-1}; no EDC; and no PPAO treatment. All further experiments were carried out on phytase immobilized on solids under those conditions.

Phytase loading rate correlated positively with aromatic content (indicated by C:H (Yang et al., 2021)) and with surface area (Fig. 2), although these correlations were not strong. Reversibility

Table 4
Zeta-potential (mV) of biochars under different conditions.

	pH = 4, EC = 10 mS cm^{-1}	pH = 5, EC = 10 mS cm^{-1}	pH = 6, EC = 10 mS cm^{-1}	pH = 7, EC = 10 mS cm^{-1}	pH = 5, EC = 20 mS cm^{-1}	pH = 5, EC = 40 mS cm^{-1}
B1	−17.05 (0.60)	−24.68 (1.25)	−27.02 (2.53)	−32.53 (2.72)	−12.46 (1.48)	−5.96 (0.57)
B2	−27.26 (0.84)	−39.10 (1.67)	−41.54 (1.45)	−41.95 (3.54)	−16.74 (1.93)	−8.35 (0.26)
B3	−5.58 (0.38)	−16.24 (0.76)	−18.30 (1.32)	−19.32 (1.83)	−7.63 (1.24)	−3.76 (0.58)
B4	−15.01 (0.29)	−33.00 (2.05)	−51.93 (1.15)	−51.01 (2.93)	−20.50 (1.33)	−10.29 (0.50)
B5	−35.03 (0.93)	−43.72 (1.87)	−45.59 (1.47)	−47.05 (2.59)	−18.67 (0.78)	−9.26 (0.35)
B6	−37.22 (0.82)	−38.09 (1.64)	−40.00 (1.04)	−41.44 (1.40)	−16.43 (0.98)	−8.14 (0.37)
B7	−9.99 (0.14)	−35.87 (1.94)	−43.60 (1.05)	−50.15 (3.46)	−19.41 (0.87)	−9.38 (0.90)
B8	−26.26 (0.85)	−40.47 (1.72)	−41.09 (3.46)	−43.60 (1.94)	−17.19 (0.74)	−8.47 (0.62)
B9	−18.48 (0.79)	−30.49 (1.90)	−39.89 (3.87)	−49.87 (3.99)	−18.95 (0.49)	−8.98 (0.88)
B1-PPAO	−18.05 (0.63)	−28.02 (1.25)	−31.59 (2.09)	−30.99 (3.16)	−12.46 (0.82)	−6.26 (0.85)
B2-PPAO	−29.49 (0.93)	−43.10 (1.88)	−45.54 (2.75)	−47.59 (2.74)	−18.83 (1.23)	−9.31 (0.94)
B3-PPAO	−9.22 (0.41)	−19.23 (0.87)	−21.05 (2.21)	−22.01 (2.51)	−8.71 (0.43)	−4.31 (0.22)
B4-PPAO	−15.01 (0.49)	−40.06 (2.29)	−58.03 (3.56)	−56.87 (3.08)	−22.86 (0.64)	−11.49 (0.40)
B5-PPAO	−38.31 (0.82)	−44.48 (2.04)	−47.15 (1.96)	−51.09 (4.15)	−20.04 (0.84)	−9.82 (0.39)
B6-PPAO	−36.26 (1.22)	−48.99 (2.42)	−60.24 (3.16)	−61.33 (2.64)	−24.42 (0.99)	−12.16 (0.63)
B7-PPAO	−10.94 (0.38)	−31.33 (1.87)	−47.29 (4.16)	−46.51 (2.97)	−18.68 (1.13)	−9.38 (0.91)
B8-PPAO	−28.73 (0.96)	−42.38 (1.95)	−46.88 (3.49)	−49.40 (3.68)	−19.51 (0.48)	−9.63 (0.72)
B9-PPAO	−27.47 (0.91)	−34.37 (1.65)	−43.55 (2.76)	−47.66 (3.45)	−18.65 (0.73)	−9.12 (0.77)

The target pH values are obtained by using MUB adjusted with HCl or NaOH. The EC values are adjusted to target values through the addition of NaCl. The numbers are expressed as mean (standard error). Abbreviations: MUB, modified universal buffer; EC, electrical conductivity; B1–B9 biochar: refer to Table 1.

tests showed that no more than 4% of the immobilized phytase detached from biochar surfaces during the seven-step, seven-day sequential extraction procedure using either dairy or poultry manure DOM solution (Fig. 3). Exhaustive extraction re-mobilized less than 50% of the phytase, regardless of the solvent used, which included ethanol, methanol, acetone, ammonium chloride solution, or a mixture of 10% ethanol in ammonium chloride, with sonication (Text S2 and Table S1).

The carboxylate resin bound around 0.6 mg phytase g^{-1} resin when EDC was included, but no detectable phytase was immobilized in the absence of EDC (Fig. S5). This indicates that these resins do not physisorb phytase well, which is consistent with their non-porous, low surface-area nature. The effects of pH and EDC dose on phytase loading were minimal.

3.3. Immobilized and remobilized phytase activity compared to phytase in free form

Phytase activity was consistently higher at pH 5 than pH 7 whether free or immobilized (Fig. 4). Immobilization, however, generally reduced phytase activity by as much as two orders of magnitude at both pH values (Fig. 4). Furthermore, the K_m value, an indicator of substrate inaccessibility, of immobilized phytase was approximately double the value of the free form in all cases (Table 6). Re-mobilized phytase was still active, although the extraction process itself reduced phytase activity to about 70% of original (Fig. S6).

Table 5
Total concentrations of selective metals in biochars.

	Cr	Fe	Mn	Co	Ni	Cu	Zn	Cd	Pb
	(mg kg^{-1})								
B1	nd	316	28.4	nd	nd	14.3	14.8	nd	nd
B2	nd	284	30.0	nd	nd	13.4	5.11	nd	nd
B3	nd	478	141	nd	nd	136	18.2	nd	nd
B4	nd	13.7	6.42	nd	nd	6.53	2.33	nd	nd
B5	nd	nd	4.93	nd	nd	nd	4.20	nd	nd
B6	nd	nd	3.07	nd	nd	0.456	5.41	nd	nd
B7	nd	135	38.3	nd	nd	38.3	62.1	nd	nd
B8	nd	127	38.1	nd	nd	23.8	21.9	nd	nd
B9	nd	nd	26.4	nd	nd	11.2	13.6	nd	nd

Abbreviations: nd, not detectable; B1–B9 biochar: refer to Table 1.

3.4. Performance of clay minerals as phytase supports

Compared to the biochar that most effectively immobilized phytase (B1), montmorillonite (specific surface area of 46.7 m^2 g^{-1}) and hematite (specific surface area of 50.3 m^2 g^{-1}) were more effective at immobilization by a factor of 2 and 1.19, respectively, while kaolinite (specific surface area of 29.3 m^2 g^{-1}) was less effecting by a factor of 0.66 (Fig. 5). However, kaolinite was best at preserving phytase activity (approximately 77–85% depending on pH), followed by hematite (34–38%), and montmorillonite (7–10%). Activity of immobilized phytase on montmorillonite was comparable to some of the biochars.

4. Discussion

4.1. Interactions between phytase and biochars

Our study finds that EDC, a commonly used agent for cross-linking —COOH and —NH_2 groups, has little effect on phytase attachment to these biochars compared to physisorption alone (control), despite that this agent is reported to successfully bind other enzymes to carboxylated carbon nanotubes (Gao and Kyratzis, 2008). The carboxylic resin, which did not physisorb phytase, can be used to estimate the contribution of EDC-mediated grafting of phytase to the biochars. The resin grafted 0.62 mg phytase per 1.11 mmol —COOH. Assuming the same ratio for the biochars, whose —COOH content ranged from 0.15–0.41 mmol g^{-1}, this means that EDC-grafted phytase amounted to 0.09–0.23 mg protein g^{-1} biochar, which is only 1–4% of the total protein bound (2.6–9.2 mg protein g^{-1} biochar). Thus, physisorption alone appears sufficient to achieve good immobilization of phytate on biochars.

Phytase is expected to bind to the biochars by a combination of electrostatic (coulombic) and hydrophobic forces. Hydrophobic effects are thought to predominate over electrostatic forces in physisorption of proteins on carbonaceous materials (Balavoine et al., 1999; Matsuura et al., 2006; Shim et al., 2002). The biochars are without exception net negatively charged at pH 4 and above, whereas phytase exhibits an isoelectric point between pH 5 and 6. Thus, the greater physisorption of phytase at pH 5 than pH 7 is consistent with a contribution of electrostatic forces. The involvement of hydrophobic effects is consistent with the positive correlation between enzyme loading and C:H ratio of the biochar. Phytase is essentially irreversibly sorbed from aqueous media, even in the presence of high manure DOM concentrations. Only partial re-mobilization

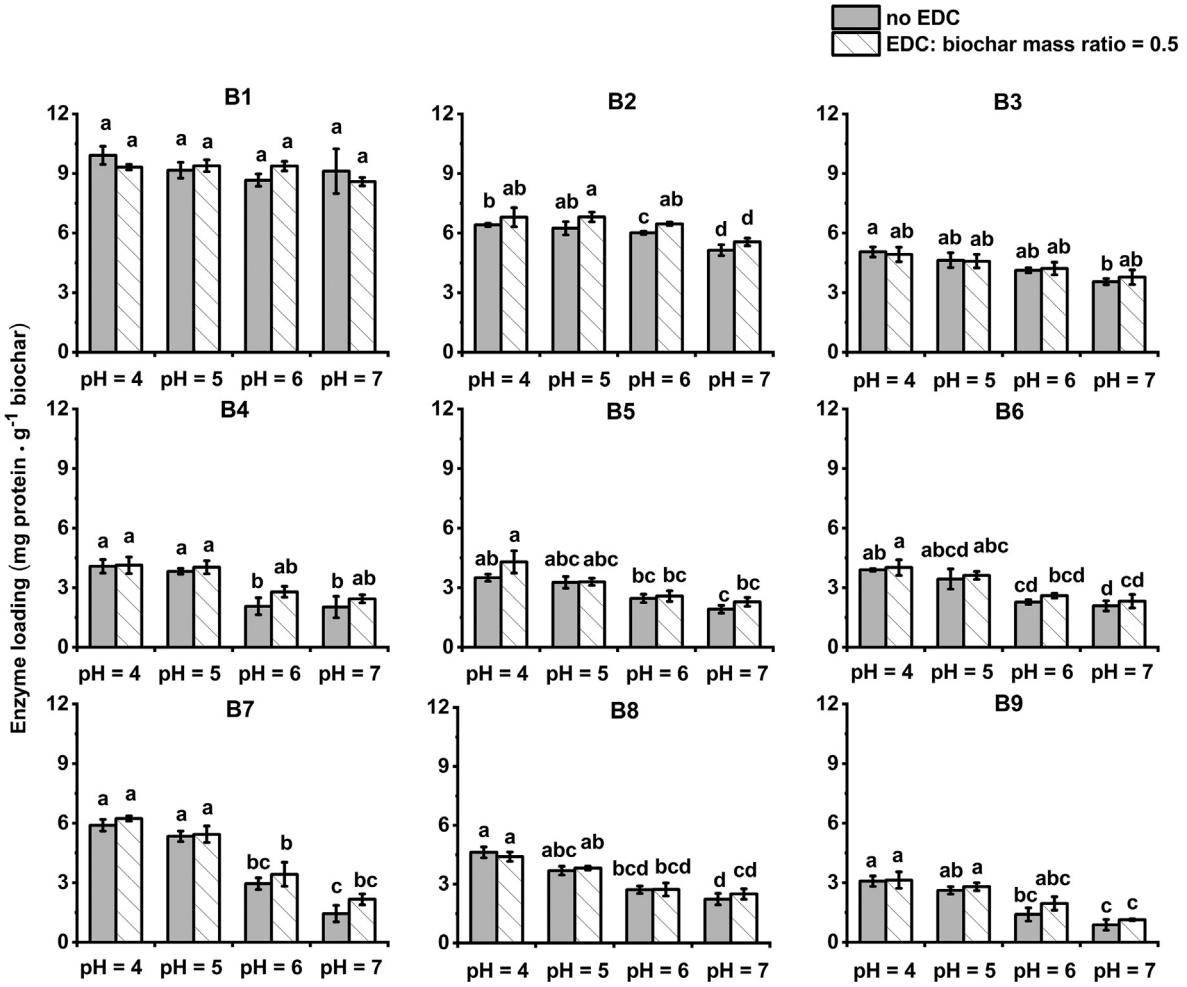

Fig. 1. Effect of pH on phytase loading amount onto different types of biochar. The phytase loading process occurs either with or without the presence of the crosslinker, EDC. All treatments are in triplicates and the values represent average ± standard error. There is no significant interaction between the pH factor and the EDC presence factor; therefore, statistical comparisons are made among different phytase loading conditions for the same type of char. Different letters on top of the bar indicate significant differences among the phytase loading conditions at a significance level of 0.05). Abbreviations: EDC: 1-ethyl-3-(3-dimethylaminopropyl) carbodiimide hydrochloride; B1–B9 biochar: refer to Table 1.

is achieved, even in organic solvents and high concentrations of ammonium salts. A likely explanation is the highly unfavorable entropy associated with detaching from multiple points of interaction with the surface before the enzyme re-enters the free state.

High ionic strength promotes aggregation of the enzyme via ion bridging, which is proposed to further limit the pores into which the enzyme can fit, and thus reduce binding (González et al., 2013; Li et al., 2010). An increase in ionic strength can also alter the zeta potential of

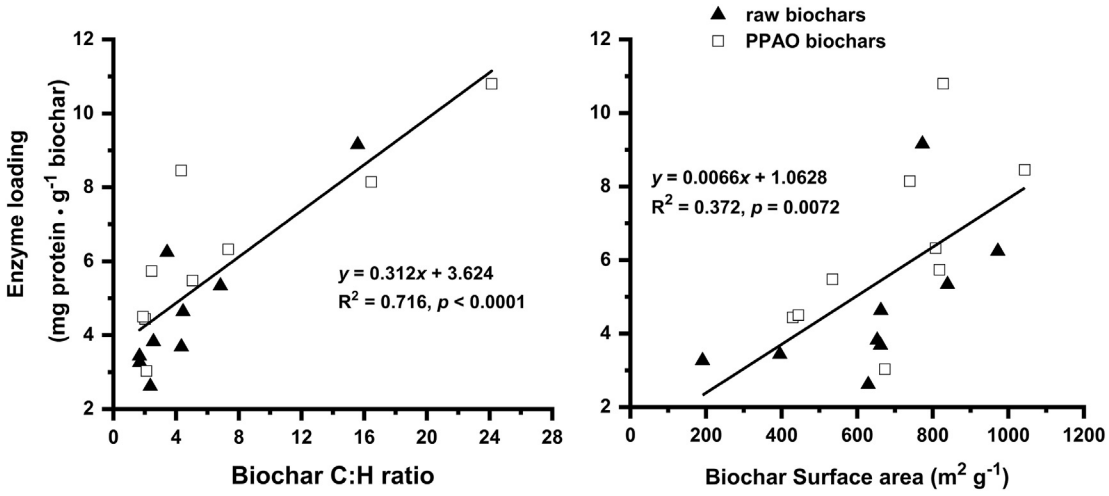

Fig. 2. Correlation between the enzyme loading amount and a) the biochar aromaticity indicator, atomic C:H ratio (left); b) the biochar specific surface area (right). Abbreviation: PPAO, post-pyrolysis air oxidation.

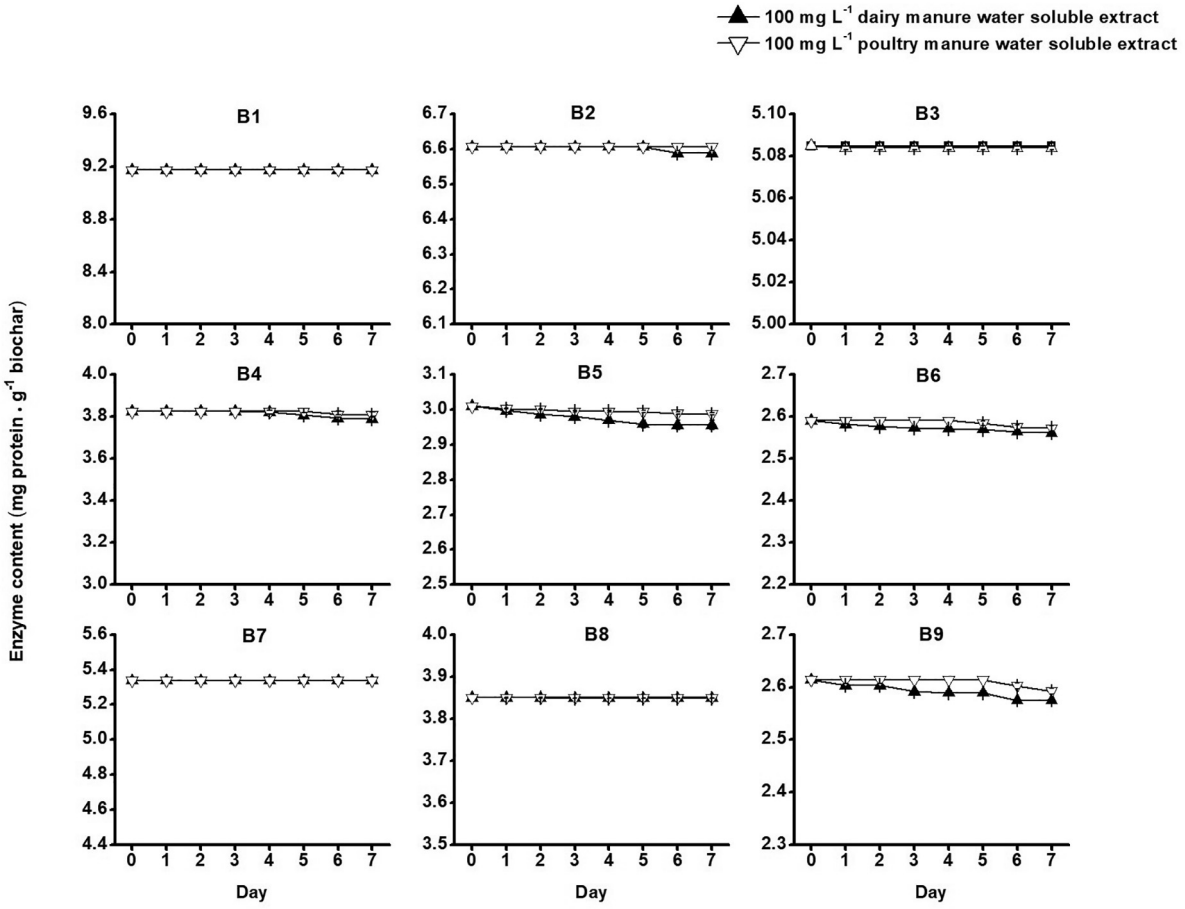

Fig. 3. Reversibility (leaching) test of immobilized phytase on the different types of biochar. Biochar adsorbed with phytase is sequentially extracted for seven days using solutions either contain dairy manure or poultry manure water extracts (both at concentrations of 100 mg extracts L^{-1}). Abbreviations: B1–B9 biochar: refer to Table 1.

the charged particles, thereby influencing the strength of electrostatic forces between phytase and biochar. For example, at pH 5, although phytase remains positively charged, the zeta potential value decreases with increasing ionic strength (Table S2), which leads to a weaker attraction towards the negatively charged biochar surface. Therefore, high concentrations of buffer should be avoided during the enzyme immobilization process.

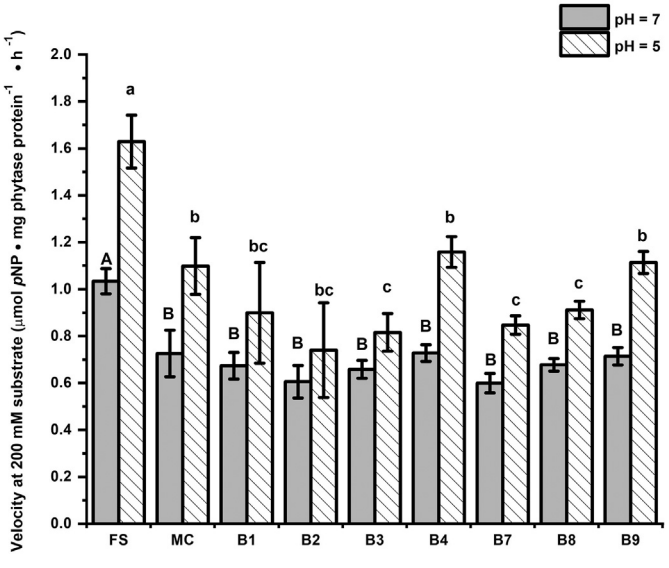

Fig. 4. Phytase activity assay of either free state or immobilized onto different types of biochar. The activity assay is performed at 25 °C with the pH of either 5 or 7 using MUB adjusted with HCl or NaOH. Detailed descriptions of the assay can be referred to Section 2.5. Abbreviations: FS, free state; MC, method control; MUB, modified universal buffer; B1–B9 biochar: refer to Table 1.

4.2. Decrease in catalytic activity of immobilized phytase

It is not uncommon to find that binding reduces enzyme activity in comparison to the free state, however our study shows that bound phytase activity is reduced by two orders of magnitude when bound to the biochars. The lower V_{max} and higher K_m of the biochar-immobilized phytase indicate a lower catalytic efficiency and a reduced substrate affinity compared to the free state. We propose three hypotheses to explain such observations. 1) The product of enzymatic reaction in the phytase assay, *p*NP, is strongly adsorbed by biochars (Table S3). Although the bound *p*NP was extractable with hot acetonitrile, it may

Table 6
K_m values of free state or immobilized phytase.

	pH = 5		pH = 7	
	K_m (mM)	R	K_m (mM)	R
Free state	16.2	0.991	19.4	0.989
B1	42.9	0.965	43.1	0.939
B2	46.4	0.970	40.7	0.961
B3	34.5	0.958	41.8	0.977
B4	38.2	0.980	39.1	0.984
B7	36.9	0.976	43.5	0.982
B8	50.7	0.960	47.1	0.952
B9	34.8	0.973	42.2	0.978

The target pH values are obtained by using MUB adjusted with HCl or NaOH. Abbreviations: MUB, modified universal buffer; B1–B9 biochar: refer to Table 1.

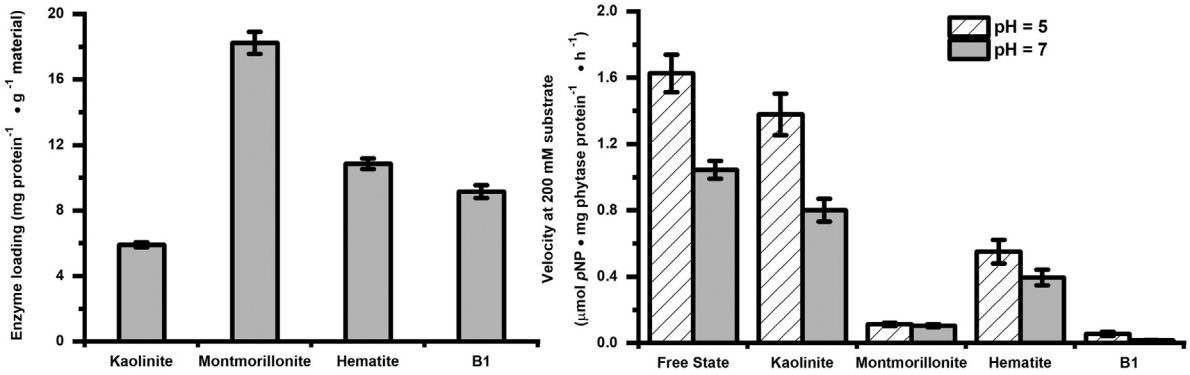

Fig. 5. Comparison of soil minerals and B1 (the biochar loaded the largest amount of phytase in this study) regarding their phytase loading rate (left) and immobilized enzyme activity (right).

have accumulated on surfaces in the vicinity of the enzyme, causing competitive inhibition (lower V_{max}) (Frieden and Walter, 1963; Purich, 2010). 2) Although not directly measured, it is deduced that the substrate *p*NPP also sorbs strongly to biochars because it is similar in molecular structure to *p*NP. Bound substrates lose freedom of mobility, which may slow their contact with bound enzyme (Allison and Jastrow, 2006; Nannipieri, 2006). 3) Reduced affinity of immobilized phytase for the substrate molecule, reflected in the higher value of K_m, may be due to conformational changes of phytase upon physisorption that alter the active site pocket.

The results suggest that enzymatic activity of phytase can be restored to its free state value once it is detached from the biochar. Therefore, endogenous chemicals on biochar surface seem not to irreversibly alter protein conformation adversely. Metals are the best-known inhibitors of enzyme activity by irreversibly masking catalytically active groups, denaturing protein conformation, or competing with metal ion cofactors (Gianfreda and Bollag, 1996). Metal ions differ in their effects; divalent cations (e.g., Co^{2+}, Mn^{2+}, Zn^{2+}, Cu^{2+} and Ni^{2+}) are usually stronger inhibitors than monovalent cations (e.g., Na^{+}) (Kumar et al., 2005; Mishra et al., 2009). Biochars used in our study contain relatively low divalent metal contents (Table 5), exposing phytase to minimal risks of irreversibly denaturation by metals.

Many studies report good performance of carbonaceous materials as enzyme supports, claiming enzyme activity as high as 92% of free-state value (Feng and Ji, 2011; González et al., 2013; Khosla et al., 2017; Naghdi et al., 2017; Taheran et al., 2017). Most of these materials are of nano size, including biochar nanoparticles, carbon nanotubes and biochar-involved nanofibrous membrane. It is possible that diffusion resistance of substrate to enzymes is lower when the enzyme is bound to nano size materials. In addition, most of these studies deal with lipases, which are inherently more active when adsorbed on hydrophobic supports because such association creates an open, substrate-accessible active site (Fernandez-Lorente et al., 2008; Fernández-Lorente et al., 2007; Hartmann and Kostrov, 2013; Palomo et al., 2002; Park et al., 2009). Phytases may not have such ability.

4.3. Comparison of clay minerals with biochars as support materials

Montmorillonite and hematite exhibit greater physisorptive affinity (Fig. 5) for phytase than biochars, even though the biochars used in this study have very large surface areas. However, most of the surface area of biochar exists in micropores (diameters <2 nm), which are too small for phytase (diameter ~3.5 nm or larger depending on ambient salinity) to penetrate. Therefore, most of the phytase was likely adsorbed on the external surfaces of the biochars (SEM images of B4 and B9 shown in Fig. S7), leading to a loading below that expected based on surface area. Meso- and macro-porous materials whose pore diameters are greater than the diameter of the enzyme molecule are reported to be better supports for enzymes than microporous materials (Li et al., 2010). Some studies have suggested that the pore diameter should be at least 1.5-fold greater than the long axis of the protein molecule (Cao, 2006; Yiu and Wright, 2005). The rank of phytase loading rate by the three minerals in our study is consistent with the order in acid phosphatase binding reported by (Shindo et al., 2002): montmorillonite > hematite > kaolinite. It is also possible the mineral surface is intrinsically more favorable for phytase adsorption than the biochar surface.

Nevertheless, phytase has lower activity on the clay minerals than in the free state. Adsorption to minerals may cause conformational changes or may favor orientation of the active site towards the surface where access to substrate may be restricted (Allison and Jastrow, 2006; Nannipieri, 2006; Quiquampoix and Burns, 2007)). Sorption of *p*NP and *p*NPP is weaker to the clays than to the biochars (Table S3) (Cervelli et al., 1973; Margenot et al., 2018). Therefore, product inhibition and/or substrate mobility may be less important for phytase activity on the clays compared to the biochars. The large decrease in phytase activity by montmorillonite follows a pattern of behavior with other enzymes (Gianfreda et al., 1992; Kelleher et al., 2004; Shindo et al., 2002).

4.4. Practical recommendations and future research direction

As a novel material used in enzyme grafting and composting processes, our study indicates a simple phytase-binding procedure when using biochar as the support; namely, physisorption. Post treatments or activations of biochars are minimally beneficial for enhancing phytase loading, and thereby can be omitted. The bound phytase has low leaching potential even in the presence of highly concentrated manure dissolved organic matter. Biochars with large pore size and high aromatic content are preferred for phytase loading. An acidic environment (pH 4 or 5) combined with low ionic strength is recommended to achieve high loading rate of phytase. However, phytase activity decreases more when bound to biochar than to some common soil minerals, indicating that for more readily available phytase activity, the inclusion of minerals, such as kaolinite or hematite, along with biochar to the composting process may provide both short- and long-term P mineralization potential.

Our study is the first to reveal that loss of enzyme activity after immobilization can be due to restricted substrate accessibility towards the enzyme, rather than irreversible damage of the enzyme protein, since a large fraction of the initial activity was recovered after extraction. Future efforts will elucidate the distribution of substrate and phytase on biochars via synchrotron radiation-based Fourier transform infrared (SR-FTIR) micro-spectroscopy.

5. Conclusions

This study shows that physisorption is sufficient to provide irreversible binding of phytase to biochars and that enzyme loading is only slightly improved by post-pyrolysis hot air oxidation pretreatment or

by including a cross-linking agent, EDC, during the immobilization. The use of PPAO and EDC cross-linking processes thus would likely not be economical considering the additional process and labor costs. Factors influencing enzyme loading and activity of the immobilized enzyme have been investigated, including pH, ionic strength (electrical conductivity), metal ion contents, hydrophobicity, and surface characteristics of both the support material and the enzyme. Exploration of these factors help understand the mechanism of immobilization and provide a basis for optimizing conditions. Although phytase immobilized on biochar shows great resistance to leaching, its activity is ~100 times lower. However, biochar may help preserve phytase in a long term since the enzyme is not irreversibly denatured and becomes active once detached from the biochar surface. Meanwhile, biochars can provide additional benefits for nutrient retention in co-composting with animal manures, and therefore the use of phytase-enriched biochars in this scenario may provide values.

CRediT authorship contribution statement

Chongyang Li: Methodology, Investigation, Writing – original draft. **Zhengyang Wang:** Investigation, Writing – review & editing. **Santanu Bakshi:** Investigation, Writing – review & editing. **Joseph J. Pignatello:** Conceptualization, Writing – review & editing, Supervision, Project administration, Funding acquisition. **Sanjai J. Parikh:** Conceptualization, Writing – review & editing, Visualization, Supervision, Project administration, Funding acquisition.

Declaration of competing interest

The authors declare that they have no known competing financial interests or personal relationships that could have appeared to influence the work reported in this paper.

Acknowledgements

This work was supported by a grant from the U.S. Department of Agriculture (USDA) National Institute of Food and Agriculture (NIFA) (Award# 2017-67019-26334). Additional support from USDA-NIFA Hatch Formula Funding and multistate regional project W-3045 is acknowledged.

Appendix A. Supplementary data

Supplementary data to this article can be found online at https://doi.org/10.1016/j.scitotenv.2021.147720.

References

Abdala, D.B., Ghosh, A.K., da Silva, I.R., de Novais, R.F., Venegas, V.H.A., 2012. Phosphorus saturation of a tropical soil and related P leaching caused by poultry litter addition. Agric. Ecosyst. Environ. 162, 15–23.
Allison, S.D., Jastrow, J.D., 2006. Activities of extracellular enzymes in physically isolated fractions of restored grassland soils. Soil Biol. Biochem. 38, 3245–3256.
Almeida, L.C., Barbosa, A.S., Fricks, A.T., Freitas, L.S., Lima, Á.S., Soares, C.M., 2017. Use of conventional or non-conventional treatments of biochar for lipase immobilization. Process Biochem. 61, 124–129.
Araji, A., Abdo, Z., Joyce, P., 2001. Efficient use of animal manure on cropland–economic analysis. Bioresour. Technol. 79, 179–191.
Bailey, V.L., Fansler, S.J., Smith, J.L., Bolton Jr., H., 2011. Reconciling apparent variability in effects of biochar amendment on soil enzyme activities by assay optimization. Soil Biol. Biochem. 43, 296–301.
Balavoine, F., Schultz, P., Richard, C., Mallouh, V., Ebbesen, T.W., Mioskowski, C., 1999. Helical crystallization of proteins on carbon nanotubes: a first step towards the development of new biosensors. Angew. Chem. Int. Ed. 38, 1912–1915.
Barnett, G., 1994. Phosphorus forms in animal manure. Bioresour. Technol. 49, 139–147.
Bradford, M.M., 1976. A rapid and sensitive method for the quantitation of microgram quantities of protein utilizing the principle of protein-dye binding. Anal. Biochem. 72, 248–254.
Brena B, Batista-Viera F. Immobilization of enzymes, from: Methods in Biotechnology: Immobilization of Enzymes and Cells. Totowa, Madrid, 2006.
Cao, L., 2006. Carrier-Bound Immobilized Enzymes: Principles, Application and Design. John Wiley & Sons.
Cervelli, S., Nannipieri, P., Ceccanti, B., Sequi, P., 1973. Michaelis constant of soil acid phosphatase. Soil Biol. Biochem. 5, 841–845.
Elzobair, K.A., Stromberger, M.E., Ippolito, J.A., 2016. Stabilizing effect of biochar on soil extracellular enzymes after a denaturing stress. Chemosphere 142, 114–119.
Feng, W., Ji, P., 2011. Enzymes immobilized on carbon nanotubes. Biotechnol. Adv. 29, 889–895.
Fernández-Lorente, G., Palomo, J.M., Cabrera, Z., Guisán, J.M., Fernández-Lafuente, R., 2007. Specificity enhancement towards hydrophobic substrates by immobilization of lipases by interfacial activation on hydrophobic supports. Enzym. Microb. Technol. 41, 565–569.
Fernandez-Lorente, G., Cabrera, Z., Godoy, C., Fernandez-Lafuente, R., Palomo, J.M., Guisan, J.M., 2008. Interfacially activated lipases against hydrophobic supports: effect of the support nature on the biocatalytic properties. Process Biochem. 43, 1061–1067.
Fidel, R.B., Laird, D.A., Thompson, M.L., 2013. Evaluation of modified Boehm titration methods for use with biochars. J. Environ. Qual. 42, 1771–1778.
Frieden, E., Walter, C., 1963. Prevalence and significance of the product inhibition of enzymes. Nature 198, 834–837.
Gao, Y., Kyratzis, I., 2008. Covalent Immobilization of Proteins on Carbon Nanotubes Using the Cross-Linker 1-Ethyl-3-(3-Dimethylaminopropyl) Carbodiimide—A Critical Assessment. ACS Publications.
Gianfreda, L., Bollag, J., 1996. Influence of natural and anthropogenic factors on enzyme activity in soil. Soil Biochem. 9.
Gianfreda, L., Rao, M., Violante, A., 1992. Adsorption, activity and kinetic properties of urease on montmorillonite, aluminium hydroxide and AL (OH) x-montmorillonite complexes. Soil Biol. Biochem. 24, 51–58.
González, M., Cea, M., Sangaletti, N., González, A., Toro, C., Diez, M., et al., 2013. Biochar derived from agricultural and forestry residual biomass: characterization and potential application for enzymes immobilization. J. Biobased Mater. Bioenerg. 7, 724–732.
Guzik, U., Hupert-Kocurek, K., Wojcieszyńska, D., 2014. Immobilization as a strategy for improving enzyme properties-application to oxidoreductases. Molecules 19, 8995–9018.
Hagemann, N., Joseph, S., Schmidt, H.-P., Kammann, C.I., Harter, J., Borch, T., et al., 2017. Organic coating on biochar explains its nutrient retention and stimulation of soil fertility. Nat. Commun. 8, 1–11.
Hartmann, M., Kostrov, X., 2013. Immobilization of enzymes on porous silicas–benefits and challenges. Chem. Soc. Rev. 42, 6277–6289.
Hudson, S., Magner, E., Cooney, J., Hodnett, B.K., 2005. Methodology for the immobilization of enzymes onto mesoporous materials. J. Phys. Chem. B 109, 19496–19506.
Igalavithana, A.D., Mandal, S., Niazi, N.K., Vithanage, M., Parikh, S.J., Mukome, F.N., et al., 2017. Advances and future directions of biochar characterization methods and applications. Crit. Rev. Environ. Sci. Technol. 47, 2275–2330.
Jensen, L.S., 2013. Animal manure fertiliser value, crop utilisation and soil quality impacts. Animal Manure Recycl. Treat. Manage. 295–328.
Jones, D., Rousk, J., Edwards-Jones, G., DeLuca, T., Murphy, D., 2012. Biochar-mediated changes in soil quality and plant growth in a three year field trial. Soil Biol. Biochem. 45, 113–124.
Jongbloed, A., Lenis, N., 1998. Environmental concerns about animal manure. J. Anim. Sci. 76, 2641–2648.
Kazenwadel, F., Wagner, H., Rapp, B., Franzreb, M., 2015. Optimization of enzyme immobilization on magnetic microparticles using 1-ethyl-3-(3-dimethylaminopropyl) carbodiimide (EDC) as a crosslinking agent. Anal. Methods 7, 10291–10298.
Kelleher, B.P., Willeford, K.O., Simpson, A.J., Simpson, M.J., Stout, R., Rafferty, A., et al., 2004. Acid phosphatase interactions with organo-mineral complexes: influence on catalytic activity. Biogeochemistry 71, 285–297.
Khadem, A., Raiesi, F., 2019. Response of soil alkaline phosphatase to biochar amendments: changes in kinetic and thermodynamic characteristics. Geoderma 337, 44–54.
Khan, A.A., Alzohairy, M.A., 2010. Recent advances and applications of immobilized enzyme technologies: a review. Res. J. Biol. Sci. 5, 565–575.
Khosla, K., Rathour, R., Maurya, R., Maheshwari, N., Gnansounou, E., Larroche, C., et al., 2017. Biodiesel production from lipid of carbon dioxide sequestrating bacterium and lipase of psychrotolerant Pseudomonas sp. ISTPL3 immobilized on biochar. Bioresour. Technol. 245, 743–750.
Kleinman, P.J., Church, C., Saporito, L.S., McGrath, J.M., Reiter, M.S., Allen, A.L., et al., 2015. Phosphorus leaching from agricultural soils of the Delmarva Peninsula, USA. J. Environ. Qual. 44, 524–534.
Kumar, S., Kikon, K., Upadhyay, A., Kanwar, S.S., Gupta, R., 2005. Production, purification, and characterization of lipase from thermophilic and alkaliphilic Bacillus coagulans BTS-3. Protein Expr. Purif. 41, 38–44.
Li, Y., Gao, F., Wei, W., Qu, J.-B., Ma, G.-H., Zhou, W.-Q., 2010. Pore size of macroporous polystyrene microspheres affects lipase immobilization. J. Mol. Catal. B Enzym. 66, 182–189.
Liang, J.F., Li, Y.T., Yang, V.C., 2000. Biomedical application of immobilized enzymes. J. Pharm. Sci. 89, 979–990.
Margenot, A.J., Nakayama, Y., Parikh, S.J., 2018. Methodological recommendations for optimizing assays of enzyme activities in soil samples. Soil Biol. Biochem. 125, 350–360.
Matsuura, K., Saito, T., Okazaki, T., Ohshima, S., Yumura, M., Iijima, S., 2006. Selectivity of water-soluble proteins in single-walled carbon nanotube dispersions. Chem. Phys. Lett. 429, 497–502.
Mishra, M.K., Kumaraguru, T., Sheelu, G., Fadnavis, N.W., 2009. Lipase activity of Lecitase® Ultra: characterization and applications in enantioselective reactions. Tetrahedron Asymmetry 20, 2854–2860.
Mohamad, N.R., Marzuki, N.H.C., Buang, N.A., Huyop, F., Wahab, R.A., 2015. An overview of technologies for immobilization of enzymes and surface analysis techniques for immobilized enzymes. Biotechnol. Biotechnol. Equip. 29, 205–220.
Naeem, I., Masood, N., Turan, V., Iqbal, M., 2021. Prospective usage of magnesium potassium phosphate cement combined with Bougainvillea alba derived biochar to reduce

Pb bioavailability in soil and its uptake by Spinacia oleracea L. Ecotoxicol. Environ. Saf. 208, 111723.
Naghdi, M., Taheran, M., Brar, S.K., Kermanshahi-pour, A., Verma, M., Surampalli, R.Y., 2017. Immobilized laccase on oxygen functionalized nanobiochars through mineral acids treatment for removal of carbamazepine. Sci. Total Environ. 584, 393–401.
Nannipieri, P., 2006. Role of stabilised enzymes in microbial ecology and enzyme extraction from soil with potential applications in soil proteomics. Nucleic Acids and Proteins in Soil. Springer, pp. 75–94.
Nguyen, L.N., Hai, F.I., Dosseto, A., Richardson, C., Price, W.E., Nghiem, L.D., 2016. Continuous adsorption and biotransformation of micropollutants by granular activated carbon-bound laccase in a packed-bed enzyme reactor. Bioresour. Technol. 210, 108–116.
Noritomi, H., Ishiyama, R., Kai, R., Iwai, D., Tanaka, M., Kato, S., 2012. Immobilization of lysozyme on biomass charcoal powder derived from plant biomass wastes. J. Biomater. Nanobiotechnol. 3, 446.
Novick, S.J., Rozzell, J.D., 2005. Immobilization of enzymes by covalent attachment. Microbial Enzymes and Biotransformations. Springer, pp. 247–271.
Palomo, J.M., Muñoz, G., Fernández-Lorente, G., Mateo, C., Fernández-Lafuente, R., Guisán, J.M., 2002. Interfacial adsorption of lipases on very hydrophobic support (octadecyl–Sepabeads): immobilization, hyperactivation and stabilization of the open form of lipases. J. Mol. Catal. B Enzym. 19, 279–286.
Panesar PS, Kumari S, Panesar R. Potential applications of immobilized β-galactosidase in food processing industries. Enzyme Res. 2010; 2010.
Park, M., Park, S.S., Selvaraj, M., Zhao, D., Ha, C.-S., 2009. Hydrophobic mesoporous materials for immobilization of enzymes. Microporous Mesoporous Mater. 124, 76–83.
Purich, D.L., 2010. Enzyme Kinetics: Catalysis and Control: A Reference of Theory and Best-Practice Methods. Elsevier.
Quiquampoix, H., Burns, R.G., 2007. Interactions between proteins and soil mineral surfaces: environmental and health consequences. Elements 3, 401–406.
Quirós, M., García, A., Montes-Morán, M., 2011. Influence of the support surface properties on the protein loading and activity of lipase/mesoporous carbon biocatalysts. Carbon 49, 406–415.
Ranganathan, S.V., Narasimhan, S.L., Muthukumar, K., 2008. An overview of enzymatic production of biodiesel. Bioresour. Technol. 99, 3975–3981.
Shahbaz, A.K., Ramzani, P.M.A., Saeed, R., Turan, V., Iqbal, M., Lewińska, K., et al., 2019. Effects of biochar and zeolite soil amendments with foliar proline spray on nickel immobilization, nutritional quality and nickel concentrations in wheat. Ecotoxicol. Environ. Saf. 173, 182–191.
Sharma, B., Dangi, A.K., Shukla, P., 2018. Contemporary enzyme based technologies for bioremediation: a review. J. Environ. Manag. 210, 10–22.
Shim, M., Shi Kam, N.W., Chen, R.J., Li, Y., Dai, H., 2002. Functionalization of carbon nanotubes for biocompatibility and biomolecular recognition. Nano Lett. 2, 285–288.
Shindo, H., Watanabe, D., Onaga, T., Urakawa, M., Nakahara, O., Huang, Q., 2002. Adsorption, activity, and kinetics of acid phosphatase as influenced by selected oxides and clay minerals. Soil Sci. Plant Nutr. 48, 763–767.
Taheran, M., Naghdi, M., Brar, S.K., Knystautas, E.J., Verma, M., Surampalli, R.Y., 2017. Degradation of chlortetracycline using immobilized laccase on Polyacrylonitrile-biochar composite nanofibrous membrane. Sci. Total Environ. 605, 315–321.
Tarafdar, J., Claassen, N., 1988. Organic phosphorus compounds as a phosphorus source for higher plants through the activity of phosphatases produced by plant roots and microorganisms. Biol. Fertil. Soils 5, 308–312.
Turan, V., 2019. Confident performance of chitosan and pistachio shell biochar on reducing Ni bioavailability in soil and plant plus improved the soil enzymatic activities, antioxidant defense system and nutritional quality of lettuce. Ecotoxicol. Environ. Saf. 183, 109594.
Turan, V., 2020. Potential of pistachio shell biochar and dicalcium phosphate combination to reduce Pb speciation in spinach, improved soil enzymatic activities, plant nutritional quality, and antioxidant defense system. Chemosphere 245, 125611.
Turan, V., Khan, S.A., Iqbal, M., Ramzani, P.M.A., Fatima, M., 2018a. Promoting the productivity and quality of brinjal aligned with heavy metals immobilization in a wastewater irrigated heavy metal polluted soil with biochar and chitosan. Ecotoxicol. Environ. Saf. 161, 409–419.
Turan, V., Ramzani, P.M.A., Ali, Q., Abbas, F., Iqbal, M., Irum, A., et al., 2018b. Alleviation of nickel toxicity and an improvement in zinc bioavailability in sunflower seed with chitosan and biochar application in pH adjusted nickel contaminated soil. Arch. Agron. Soil Sci. 64, 1053–1067.
Turner, B.L., 2010. Variation in pH optima of hydrolytic enzyme activities in tropical rain forest soils. Appl. Environ. Microbiol. 76, 6485–6493.
Vinu, A., Miyahara, M., Ariga, K., 2005. Biomaterial immobilization in nanoporous carbon molecular sieves: influence of solution pH, pore volume, and pore diameter. J. Phys. Chem. B 109, 6436–6441.
Wang, Z., Bakshi, S., Li, C., Parikh, S.J., Hsieh, H.-S., Pignatello, J.J., 2020. Modification of pyrogenic carbons for phosphate sorption through binding of a cationic polymer. J. Colloid Interface Sci. 579, 258–268.
Xiao, F., Pignatello, J.J., 2016. Effects of post-pyrolysis air oxidation of biomass chars on adsorption of neutral and ionizable compounds. Environ. Sci. Technol. 50, 6276–6283.
Xiao, F., Bedane, A.H., Zhao, J.X., Mann, M.D., Pignatello, J.J., 2018. Thermal air oxidation changes surface and adsorptive properties of black carbon (char/biochar). Sci. Total Environ. 618, 276–283.
Yang, J., Pignatello, J.J., Pan, B., Xing, B., 2017. Degradation of p-nitrophenol by lignin and cellulose chars: H2O2-mediated reaction and direct reaction with the char. Environ. Sci. Technol. 51, 8972–8980.
Yang, J., Pignatello, J.J., Yang, K., Wu, W., Lu, G., Zhang, L., et al., 2021. Adsorption of organic compounds by biomass chars: direct role of aromatic condensation (ring cluster size) revealed by experimental and theoretical studies. Environ. Sci. Technol. 55, 1594–1603.
Yiu, H.H., Wright, P.A., 2005. Enzymes supported on ordered mesoporous solids: a special case of an inorganic–organic hybrid. J. Mater. Chem. 15, 3690–3700.